Linear ubiquitination of LKB1 activates AMPK pathway to inhibit NLRP3 inflammasome response and reduce chondrocyte pyroptosis in osteoarthritis

Yang Chen [a,b], Yiheng Liu [b], Kai Jiang [c], Zi Wen [a], Xu Cao [a,d,*], Song Wu [a,**]

[a] Department of Orthopedics, Third Xiangya Hospital of Central South University, Changsha, 410013, China
[b] Department of Orthopedics, Haikou People's Hospital/Haikou Affiliated Hospital of Central South University, Xiangya School of Medicine, Hai Kou, 570100, China
[c] Department of Orthopedics, Second Xiangya Hospital of Central South University, Changsha, 410011, China
[d] Institute of Basic Medicine and Cancer (IBMC), Chinese Academy of Sciences, Hangzhou, 310022, China

ABSTRACT

Background: Osteoarthritis (OA) is the most common chronic disease. It is characterized by high levels of clinical heterogeneity and low inflammation. Therefore, elucidation of the mechanisms that regulate gene expression is critical for developing effective OA therapies. This study aimed to explore the role of LKB1/AMPK in the progression of OA.
Methods: Anterior cruciate ligament transection (ACLT) was performed on Sprague Dawley (SD) rats right knee to construct OA model, followed by AICAR [AMP-activated protein kinase (AMPK) activator] treatment. The level changes [AMPK, IL-10, IL-13, IL-1β, TNF-α, IL-6, ASC, Caspase-1, Ki67, and hibit Nod-like receptor protein 3 (NLRP3)] and the degree of tissue injury were assessed by western blot, Immunohistochemical (IHC), Enzyme-linked immunosorbent assay (ELISA), Hematoxylin-eosin staining (HE), Immunofluorescence (IF), Terminal deoxynucleotidyl transferase dUTP nick-end labeling (TUNEL) assay, and Safranin O and Fast Green staining (S–O). Human chondrocytes were induced by LPS to construct a cellular inflammatory model, and then transfected with oe-AMPK or oe-HOIL-1–interacting protein (HOIP). Cell viability/apoptotic and intracellular content of AMPK, HOIP, IL-1β, IL-10, IL-13, TNF-α, IL-6, ASC, NLRP3 and Caspase-1 were measured by western blot, ELISA, CCK-8, IF, flow cytometry and TUNEL assays.
Results: After AICAR treatment with OA rats, the expression of p-AMPK, IL-10, IL-13, Ki67 and Bcl-2 increased, the level of NLRP3 inflammasome, TNF-α, IL-6, Bax and Caspase-3 levels were decreased, and tissue damage and apoptosis were significantly alleviated. After transfected with oe-LKB1, chondrocyte activity and LKB1 linear ubiquitination were enhanced, and the level of HOIP, p-AMPK, IL-10 and IL-13 were increased. In contrast, NLRP3 inflammasome (ASC, NLRP3, Caspase-1, IL-1β, and cleaved Caspase-1), TNF-α, and IL-6 levels decreased, apoptosis rate and TUNEL positive rate were attenuated.
Conclusion: LKB1/AMPK pathway significantly ameliorated NLRP3 inflammasome response and chondrocyte injury. Activation of AMPK pathway by linear ubiquitination of LKB1 may be a potential target for OA treatment.
The translational potential of this article: This study highlights the importance of the LKB1/AMPK pathway in NLRP3 inflammatory body response and chondrocyte injury. Activation of LKB1 by modulating linear ubiquitination may be a potential target for OA treatment.

1. Introduction

Osteoarthritis (OA) is a degenerative disease characterized by high levels of clinical heterogeneity and low inflammation [1,2]. The current treatment options do not provide satisfactory outcomes for patients. OA progression and cartilage degeneration were influenced by abnormal metabolic responses of chondrocytes in the changes of inflammatory microenvironment [3]. It is important to explore the mechanism of extracellular matrix (ECM) degradation regulation for OA treatment [4]. Interesting, LKB1 was essential for inhibiting catabolic responses of stroma and maintaining AMPK activity in chondrocytes [5]. As a key bioenergy sensor, AMPK mediates energy homeostasis and REDOX

balance in chondrocytes to resist cellular stresses [6,7].

Furthermore, abnormal AMPK activity was connected to decreased autophagy and joint tissue inflammation [8]. Besides, simultaneous fluctuation of LKB1 and AMP-activated protein kinase (AMPK) activity was associated with senescence and biomechanical damage [9]. These abnormalities eventually lead to synovial inflammation and the abnormal of subchondral bone [8]. Modulating LKB1 or AMPK activity may be a new strategy to treat OA.

AMPK pharmacological activator attenuates IL-1β and TNF-α proteolitical cleavage in cartilage explants and monolayer chondrocytes [10]. Metformin effectively alleviates cartilage degeneration and aging by regulating AMPK/mTOR signaling pathway [11]. Therefore, decreased AMPK activity may disrupt cartilage homeostasis by influencing stromal catabolism to promote the development of OA [3,12]. Besides, AMPK has been reported to inhibit Nod-like receptor protein 3 (NLRP3) by activating autophagy [13,14]. Thus, this study was aimed to determine the influence of NLRP3 inflammasome through the AMPK/mTOR pathway.

The regulation of OA progression is also affected by pyroptosis [15]. Pyroptosis induces cell lysis, resulting in the massive release of pro-inflammatory factors and cellular contents. This promotes the development of many autoimmune and inflammatory diseases [15]. Pyroptosis was a programmed cell death signaling pathway required by Caspase-1 [16,17]. It leads to the production of IL-1β and the lysis of macrophages [18,19]. Besides, the process of pyroptosis was pro-inflammatory and mediated by NLRP3 inflammasome and Caspase-1 signaling [20]. Moreover, linear ubiquitination in vivo is associated with preventing inflammation and regulating immune signaling [21].

Therefore, we hypothesized that linear ubiquitination of LKB1, AMPK and NLRP3 mutually regulate the progression of OA.

2. Materials and methods

2.1. Establishment of OA rat models

Male Sprague Dawley rats (8 weeks of age) were reared in 12 h light/ darkness and adapted for 7 days. Next, the rats were divided into four groups randomly. In the Sham group (Sham, n = 6), only surgical incisions were made in the rats' right knee capsules. In the OA group (OA, n = 6), anterior cruciate ligament transection (ACLT) was performed on the rats' right knee [22,23]. The next day after ACLT, we constructed two other groups of rats. In the OA + NC group (OA + NC, n = 6), OA rats' articular cavities were injected with 0.4 mL normal saline every day for 7 consecutive days. In the OA + AICAR group (OA + AICAR, n = 6), Each rat was injected with 100 mg/kg AICAR (A9978-5 MG, Sigma, USA). for 7 consecutive days [24].

All rats were anesthetized with 2% isoflurane inhalation during surgery. Serum and cartilage tissue of rats were collected for subsequent detection. The serum was tested by Enzyme-linked immunosorbent assay (ELISA). After the OARSI score, the cartilage tissues were detected by western blot, Immunohistochemical (IHC), Hematoxylin-eosin staining (HE), Safranin O and Fast Green staining (S–O), Quantitative real-time polymerase chain reaction (qRT-PCR), and Terminal deoxynucleotidyl transferase dUTP nick-end labeling (TUNEL) assay.

2.2. Cell treatment

Human Chondrocytes (American Type Culture Collection, USA) in DMEM medium containing 10% FBS (PM150312B, Yaji Biotechnology Co., Ltd., China) in a 37 °C incubator supplied with 5% CO2. Next, cells were induced by 100 ng/mL LPS for 1 h [25]. Subsequently, LPS-induced model cells were transfected. The overexpression sequence (oe) of LKB1, HOIL-1–interacting protein (HOIP) and AMPK, and negative control (oe-NC) were transfected into chondrocytes by Lipofectamine™ 2000 kit (Baimaige Biotechnology Co., Ltd., Wuxi, China, 11668019) respectively. The executed operation steps were according to the kit instructions.

Cell supernatants and cells were collected for subsequent testing. Cell supernatants were tested by ELISA. The cells were detected by Cell Counting Kit-8 (CCK-8), qRT-PCR, western blot, Co-Immunoprecipitation (CO-IP), Immunofluorescence (IF), TUNEL, and flow cytometry.

2.3. IHC

After the OARSI score, the cartilage tissues were detected by IHC. In short, slices were dewaxed and dehydrated first. Slices were soaked in 0.01 M citrate buffer at high temperature for 20 min and cooled to room temperature. Next, slices were put in 3% H2O2 for 10 min after being cleaned with PBS. The p-LKB1 primary antibody (PA5-105896, 1:100, Thermo Fisher, USA), p-AMPK primary antibody (PA5-36615, 1:100, Thermo Fisher, USA), Ki67 primary antibody (27309-1-AP, 1:100, PTG, USA), NLRP3 primary antibody (19771-1-AP, 1:100, PTG, USA), and ASC primary antibody (10500-1-AP, 1:100, PTG, USA) were incubated. Next, the corresponding secondary antibody was mixed and incubated for 30 min. We dropped the DAB working solution and incubated it for 5–10 min at room temperature. After dehydration by alcohol, the tablets were placed in xylene, sealed with neutral gum, and observed under a microscope.

2.4. CO-IP

CO-IP was used to detect the cells. IP lysis buffer (#AWB0144, Abiowell, China) was applied to lysed cells. Cells were treated with IP lysis buffer for 1.5 min after sonication and continued to be treated at low temperature for 30 min. Subsequently, the supernatant after centrifugation at 12000 rpm was collected. Next, cells were incubated with antibodies against LKB1 (10746-1-AP, Proteintech, USA) and normal rabbit IgG (B900620, Proteintech, USA) at 4 °C overnight. Cell lysates were then combined with protein A/G agarose beads (#9863, Cell Signaling Technology, USA) for 2 h. Subsequently, collected precipitates were washed with ice IP buffer and analyzed by western blot.

2.5. ELISA

Serum and cell supernatants were tested by ELISA, respectively. To measure the content of inflammatory factors, IL-1β (# CSB-E08055r, CUSABIO, China), TNF-α (# CSB-E11987r, CUSABIO, China), IL-6 (# CSB-E04640r, CUSABIO, China), IL-10 (# CSB-E04595r, CUSABIO, China), and IL-13 (# CSB-E07454r, CUSABIO, China) ELISA kits were utilized. After the reagents had been left at room temperature for 30 min, the reagents were prepared according to the instructions. Subsequently, the samples and reagents were added sequentially according to the desired criteria. After color-developing at 37 °C for 15–30 min, the stop solution was added to the well and reacted for 5 min. The Optical Density (OD) value was collected by Bio-Tek microplate reader (MB-530, Heales, China), and the concentration was calculated regarding the standard curve.

2.6. IF

The cells were detected by IF. Firstly, the distribution and level of NLRP3 and Caspase-1 were detected by IF. 4% paraformaldehyde was applied to fix cells for 30 min. The cells were infiltrated with 0.1% TritonX-100 to permeate the cell membrane after washing with PBS. Next, BSA was applied to block the nonspecific antigen at 25 °C and spent the night on anti- NLRP3 antibody (19771-1-AP, PTG) or anti-Caspase-1 antibody (MA5-32909, Thermo Fisher) at 4 °C. After PBS washing, secondary bodies Anti-Rabbit IgG (H + L) were applied to culture the cells. The nucleus was incubated with DAPI. Finally, cells were observed under a fluorescence microscope (BA210T, Motic, China).

Table 1
The information of antibody.

Name	Article number	Source	Dilution rate	Molecular weight	Transfer film time	Company
AMPK	10929-2-AP	Rabbit	1:500	64 kDa	85 min	Proteintech (UAS)
P-AMPK	PA5-36615	Rabbit	1:1000	63 kDa	85 min	Thermo Fisher (UAS)
NF-kB	10745-1-AP	Rabbit	1:2000	65 kDa	85 min	Proteintech (UAS)
Caspase-1	22915-1-AP	Rabbit	1:5000	45-47/30–35 kDa	60 min	Proteintech (UAS)
cleaved-Caspase-1	ab179515	Rabbit	1:1000	10/12 kDa	30 min	Abcam (UK)
HOIP	PA5-115849	Rabbit	1:1000	≈100 kDa	120 min	Thermo Fisher (UAS)
NLRP3	19771-1-AP	Rabbit	1:800	110 kDa	125 min	Proteintech (UAS)
ASC	10500-1-AP	Rabbit	1:3000	22–25 kDa	45 min	Proteintech (UAS)
IL-1β	ab254360	Rabbit	1:1000	≈30 kDa	55 min	Abcam (UK)
LKB1	10746-1-AP	Rabbit	1:100	54 kDa	75 min	Proteintech (UAS)
p-LKB1	PA5-105896	Rabbit	1:2000	≈50–70 kDa	90 min	Thermo Fisher (UAS)
Bcl2	12789-1-AP	Rabbit	1:2000	25–30 kDa	55 min	Proteintech (UAS)
Bax	50599-2-Ig	Rabbit	1:1000	21 kDa	45 min	Proteintech (UAS)
Caspase-3	19677-1-AP	Rabbit	1:5000	17/19/32–35 kDa	55 min	Proteintech (UAS)
β-actin	66009-1-Ig	Mouse	1:5000	42 kDa	60 min	Proteintech (UAS)
HRP goat anti-Rabbit IgG	SA00001-2	Rabbit	1:6000	/	90 mim	Proteintech (UAS)
HRP goat anti-mouse IgG	SA00001-1	Mouse	1:5000	/	90 mim	Proteintech (UAS)

2.7. HE

After the OARSI score, the cartilage tissues were detected by HE. HE staining was performed regarding routine protocols [17]. After deparaffinization and rehydration, 5 μm longitudinal sections were stained with hematoxylin solution for 5 min. Next, the sections were dipped in 1% acid ethanol for 5 times. Then eosin solution was applied to stain the sections for 3 min. The sections were dehydrated with graded alcohol. The mounted slides were photographed using a fluorescence microscope.

2.8. S–O

After the OARSI score, the cartilage tissues were detected by S–O. Knee joint samples were fixed in paraformaldehyde for 24 h and decalcified in 10% EDTA solution for 2 weeks. Next, the samples were dehydrated by graded alcohol and embedded in paraffin blocks. Frontal serial sections (4-μm thick) across the entire joint were obtained, and slides were selected and stained with S–O solution to detect cartilage destruction. The images were captured digitally by a microscope. Besides, S–O staining was applied for Osteoarthritis Research Society International (OARSI) scoring [26].

2.9. CCK-8

Human Chondrocytes in each group were cultured with 5×10^3 cells/100 μL into 96-well plates for 24 h. Each group is provided with 3 multiple holes. Next, 10 μL CCK-8 Working Solution (NU679, DOJINDO) was added to each well. After incubation for 4 h in 37 °C, the absorbance value (450 nm) was measured with a microplate reader.

2.10. TUNEL assay

The cells and cartilage tissues were detected by TUNEL, respectively. TUNEL Apoptosis Assay Kit (40306ES50, Yeasen Biotechnology) was applied to detect the apoptosis rate. The cleaned slipper was fixed with paraformaldehyde for 30 min and cleaned again. The Proteinase K working solution was treated for 20 min. Subsequently, the slides were dripped with the Equilibration Buffer until soaked and incubated for 30 min. After absorbing part of the liquid, TdT incubation buffer solution and DAPI working solution were successively added. Before adding DAPI working solution, tissue-derived sections needed to be reacted with Streptavidin-TRITC labeled working solution for 30min at 37 °C in the dark. This procedure is not required for cell-derived sections. The slippers were detected under a fluorescence microscope after being shielded from light.

2.11. Flow cytometry

The cells apoptosis were detected by flow cytometry. First, the cells were collected with Trypsin solution without EDTA (C0201, Beyotime, China). Next , the collected cells were washed with PBS for once. The cells were treated with Annexin V-FITC Apoptosis Detection Kit (KGA108, NanJing KeyGen Biotech). Briefly, Binding Buffer was applied to suspend cells. Next, Annexin V-FITC and Propidium Iodide were used to treat cells for 10 min. A flow cytometer (A00-1-1102, Beckman, USA) was used for the next measurement and calculation. The experiments were independently repeated 3 times.

2.12. Western blot

The cells and cartilage tissues were detected by western blot, respectively. To cells, 200 uL of RIPA lysate was added to cells washed with ice-precooled PBS. The cells were scraped off with a cell scraper and broken by ultrasound for 1.5min. The cells were then kept at a low temperature and lysed for 10 min. After centrifugation at 12000 rpm for 15 min, the supernatant was collected. To cartilage tissues, 300 uLRIPA lysate was added to 0.025 g tissue. The tissue was ground repeatedly until no tissue was visible. The tissue fluid was further lysed at a low temperature for 10 min. After centrifugation at 12000 rpm for 15 min, the supernatant was collected.

The content of proteins was measured by the BCA protein kit. Each well was filled with denatured protein. After the gel reached the bottom, electrophoresis was terminated. Next, the transfer buffer solution was placed with Gel, filter paper and NC membrane in turn, and the membrane was transferred at a constant current. PBST (5% skimmed milk) powder was applied to dispose of the membrane for 1.5 h. Next, the first and secondary antibodies were added to the membrane. The chemiluminescence imaging system calculated the protein samples on the membrane. β-actin was carried to display as an internal reference. The antibody information was shown in Table 1.

2.13. qRT-PCR

The cartilage tissues and cells were detected by qRT-PCR. Trizol Reagent (15596018, Invitrogen, USA) was applied to extract total RNA. After 1 mL Trizol Reagent was added to 0.02 g of tissue or 500 μL of cells, the cells or tissue were lysed for 3 min at room temperature. Revert Aid First Strand cDNA Synthesis Kit (CW2569, Beijing Comwin Biotech, China) was used to reversely transcribed cDNA. The primer sequences of NLRP3, Caspase-1, Caspase-3, ASC, IL-1β, Bcl-2, Bax, and β-actin were provided by Sangon Biotech (Table 2). Then, DNA amplification and detection were analyzed with a fluorescent quantitative PCR instrument

Table 2
The primer sequence.

Primer ID	5′-3′
β-actin-F	ACATCCGTAAAGACCTCTATGCC
β-actin-R	TACTCCTGCTTGCTGATCCAC
NLRP3-F	CACCTCTTCTCTGCCTACCTG
NLRP3-R	AGCTGTAAAATCTCTCGCAGT
Caspase-1-F	CTAGACTACAGATGCCAACCAC
Caspase-1-R	GGCTTCTTATTGGCATGATTCCC
ASC-R	CCCTGTCCCGTTCTCATACCG
ASC-R	CAAACACCAAAAGGCAACAAGCA
IL-1β-F	CAGCAGCATCTCGACAAGAG
IL-1β-R	AAAGAAGGTGCTTGGGTCCT
Bcl-2-F	CTGGTGGACAACATCGCTCT
Bcl-2-R	ATAGTTCCACAAAGGCATCCCA
Bax-F	TTGCTACAGGGTTTCATCCAGG
Bax-R	GCTCCAAGGTCAGCTCAGGT
Caspase-3-F	ATCAGCCTAATTTTACAGACC
Caspase-3-R	TCTCCTTTCCTTACGCTCT

(PIKOREAL96, Thermo Fisher, USA). 2-△△CT was applied to assess the relative mRNA level. β-actin acted as reference.

2.14. Statistical analysis

Graphpad Prism 9 was used for statistical analysis. The data were represented as the mean ± standard deviation ($\overline{X}$ ± SD). Student's T-test was used to analyze the differences between the two groups, and one-way analysis of variance (ANOVA) was used to compare the data differences between multiple groups. P-value < 0.05 was considered statistically significant.

3. Results

3.1. LKB1 mediated AMPK activation in chondrocytes

Western blot and IHC results of ACLT constructed OA rats showed no significant changes in AMPK and LKB1 protein contents, while p-AMPK and p-LKB1 protein contents decreased (Fig. 1A and B). After LKB1 overexpression treatment, the levels of p-AMPK and p-LKB1 protein increased (Fig. 1C), and the levels of NF-κB and Caspase-1/cleaved Caspase-1 decreased (Fig. 1D). These studies demonstrated that p-LKB1 content decreased in OA chondrocytes, and LKB1 mediated the activation of AMPK in chondrocytes.

3.2. Linear ubiquitin modification promoted LKB1 activity and increased AMPK activation

The levels of LKB1 in K48, K63 and M1 (linear ubiquitination) were detected by immunoprecipitation. LKB1 has no obvious precipitation in
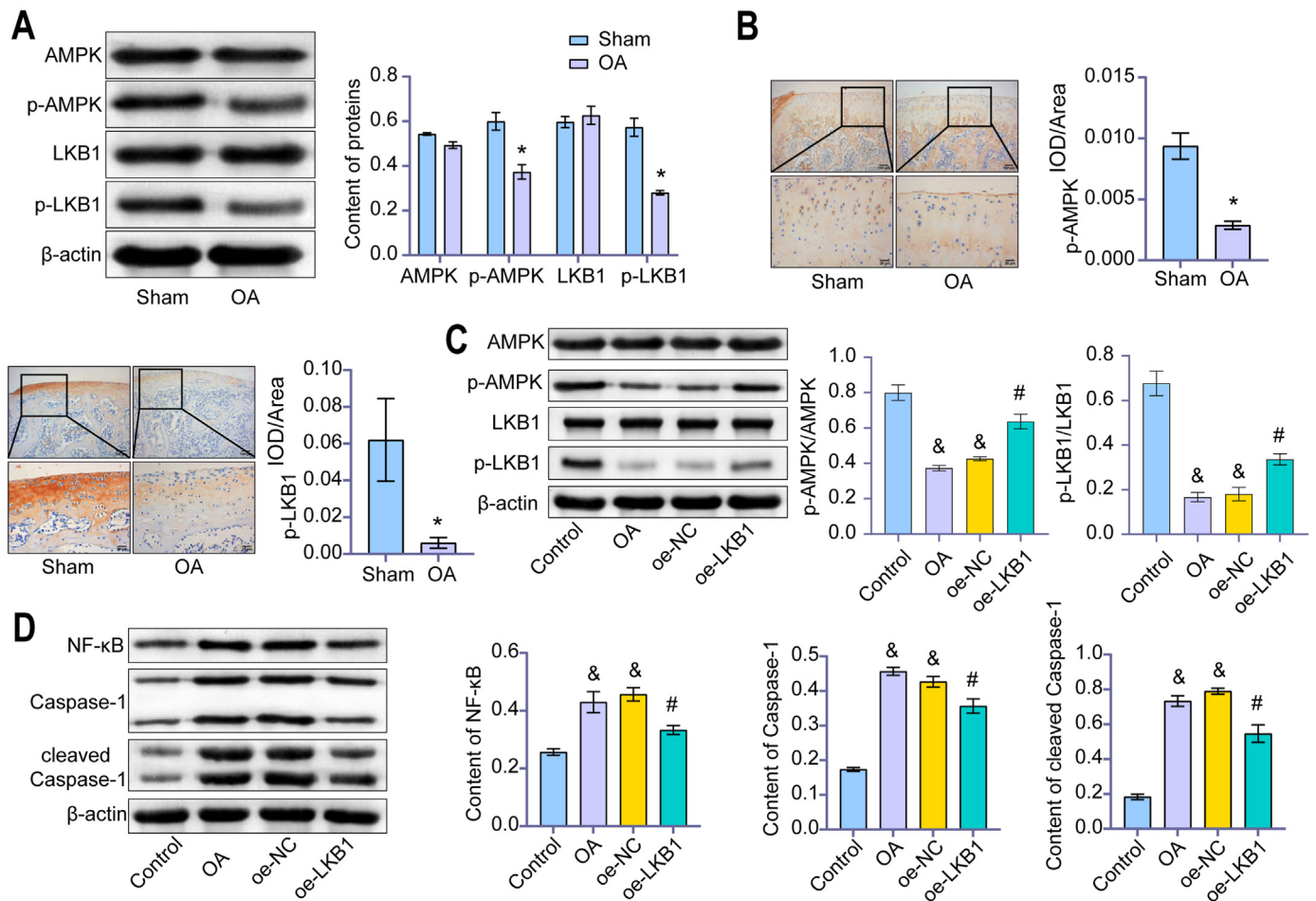

Figure 1. LKB1 mediated AMPK activation in chondrocytes. (A) Western blot was applied to measure the content of AMPK, LKB1, p-AMPK and p-LKB1. (B). IHC was applied to measure IOD/Area of p-AMPK and p-LKB1 (IHC, × 400, scale bar = 25 μm; × 100, scale bar = 100 μm). There were no significant changes in AMPK and LKB1 protein contents, while p-AMPK and p-LKB1 protein contents decreased in OA rats. (C) Content of AMPK, p-AMPK, LKB1, and p-LKB1 were detected by western blot. After LKB1 overexpression treatment, the levels of p-AMPK and p-LKB1 protein increased. (D) Content of NF-κB, Caspase-1 and cleaved Caspase-1 were detected by western blot. After LKB1 overexpression treatment, the levels of NF-κB and Caspase-1/cleaved Caspase-1 decreased. *P < 0.05 vs. Sham. & P < 0.05 vs. Control. #P < 0.05 vs. LPS + oe-NC.
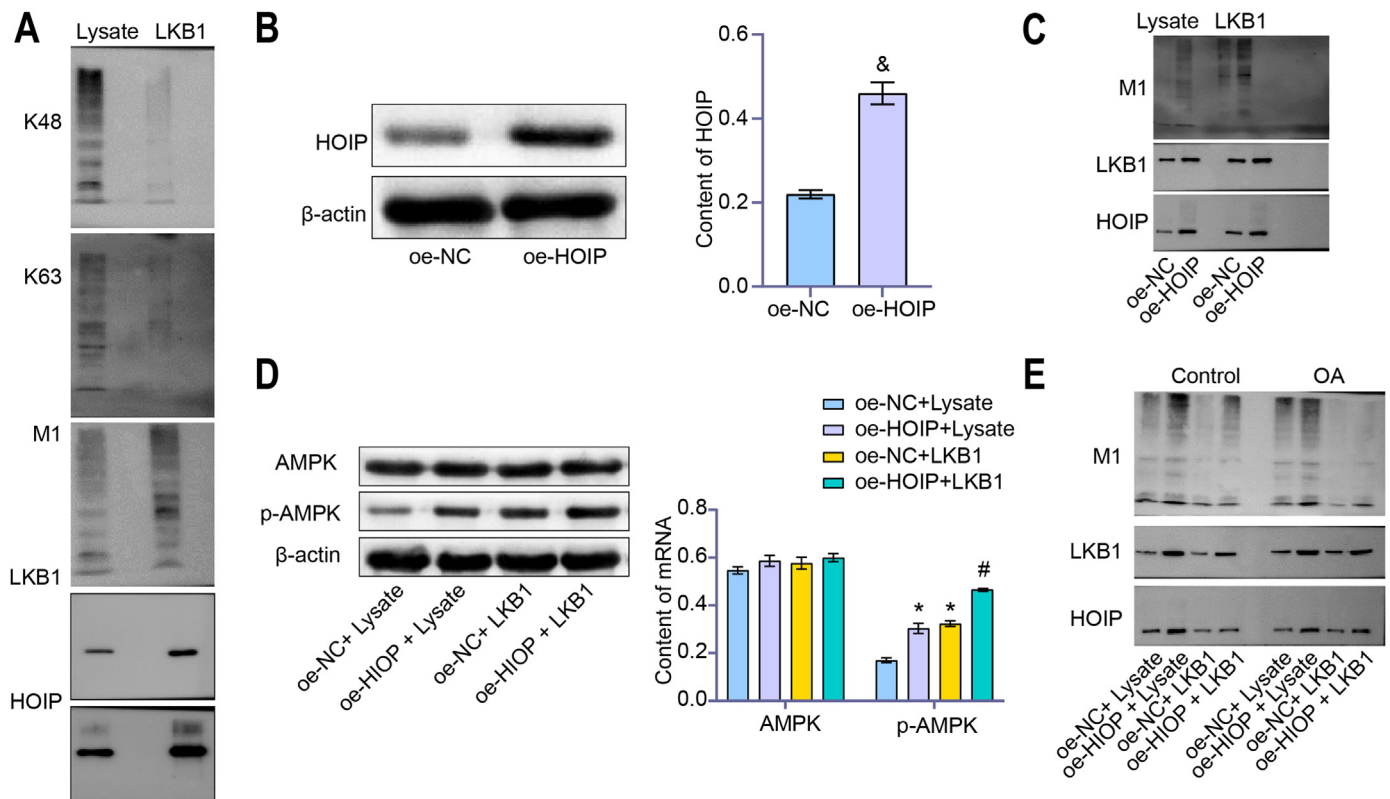
Figure 2. Linear ubiquitin modification promoted LKB1 activity and increased AMPK activation. (A) LKB1 was detected by immunoprecipitation in K48, K63 and M1 (linear ubiquitination). LKB1 has no obvious precipitation in K48 and K63, but was precipitated in M1. (B) Western blot was used to detect HOIP content. HOIP expression of LPS + oe-HIOP was increased compared with that of LPS + oe-NC group. (C) Linear ubiquitin modification of LKB1 was detected by immunoprecipitation M1-Ub (D) AMPK and p-AMPK contents were detected by western blot. In Lysate or LKB1 treated groups, linear ubiquitination of LKB1 was enhanced after overexpression of HOIP. And expressions of HOIP and p-AMPK were increased, with no significant difference in AMPK. (E) Linear ubiquitin modification of LKB1 in chondrocytes was detected by immunoprecipitation M1-Ub. Expression of LKB1 and HOIP increased after overexpression of HOIP in the Control and LPS groups. & $P < 0.05$ vs. oe-NC. *$P < 0.05$ vs. oe-NC + Lysate. #$P < 0.05$ vs. oe-NC + LKB1.

K48 and K63, but was precipitated in M1 (Fig. 2A). HOIP expression of LPS + oe-HIOP was increased compared with that of LPS + oe-NC group, indicating successful construction of overexpressed HIOP (Fig. 2B). In the LKB1 treated groups, linear ubiquitination of LKB1 was enhanced after overexpression of HOIP. And the expressions of HOIP and p-AMPK were increased, with no significant difference in AMPK (Fig. 2C and D). Expression of LKB1 and HOIP increased after overexpression of HOIP in the Control and LPS groups (Fig. 2E). These results suggested that linear ubiquitin modification promotes LKB1 activity and increases AMPK activation.

3.3. AMPK inhibited NLRP3 inflammatory response of chondrocytes in OA

We found AICAR (AMPK activator) reversed the increase of the OARSI score of rats induced by OA (Fig. 3A). This indicated that we successfully induced the ACLT rats model. After treatment with AICAR, the expression of p-AMPK increased in chondrocytes of rats induced by OA, but there was no significant difference in AMPK (Fig. 3B). AICAR treatment significantly down-regulated the levels of IL-1β, TNF-α and IL-6, and increased the levels of IL-10 and IL-13 (Fig. 3C). In addition, AICAR treatment significantly down-regulated the expression of the NLRP3 inflammasome (ASC, Caspase-1, IL-1β, NLRP3, and cleaved Caspase-1) in OA rats (Fig. 3D). IHC results also showed that AICAR treatment significantly down-regulated NLRP3 and ASC expression (Fig. 3E). These results demonstrated that AMPK inhibited the NLRP3 inflammatory response of OA chondrocytes.

3.4. AMPK regulated NLRP3 inflammatory response of chondrocytes in OA to inhibit pyroptosis

After LPS-induced human chondrocytes constructed an inflammatory model, the level of p-AMPK decreased in the LPS group. Compared with the LPS group, the level of p-AMPK in the LPS + oe-AMPK group was higher (Fig. 4A). CCK-8 showed cell viability of the LPS group was decreased compared with the Control group. Overexpression of AMPK up-regulated cell viability (Fig. 4B). The levels of IL-1β, TNF-α and IL-6 in the LPS group were higher than in the control group, while the levels of IL-10 and IL-13 were lower than in the control group. Overexpression of AMPK significantly up-regulated the levels of IL-10 and IL-13 and down-regulated the levels of IL-1β, TNF-α and IL-6 (Fig. 4C). In addition, overexpression of AMPK down-regulated the expression of NLRP3 inflammasomes ASC, Caspase-1, IL-1β, NLRP3, and cleaved Caspase-1 (Fig. 4D–F). Moreover, the apoptosis and TUNEL positive rates decreased (Fig. 4G and H). These studies demonstrated that AMPK reduced the NLRP3 inflammatory response of chondrocytes and inhibited pyroptosis.

3.5. AMPK reduced chondrocyte injury in OA rats

HE and S–O pathological results showed that the OA group's injury degree increased under the Sham group's comparison. AICAR treatment significantly alleviated tissue damage (Fig. 5A and B). Compared with the Sham group, the Bcl-2 level was down-regulated, and the level of Bax and Caspase-3 was up-regulated in OA group. Compared with the OA + NC
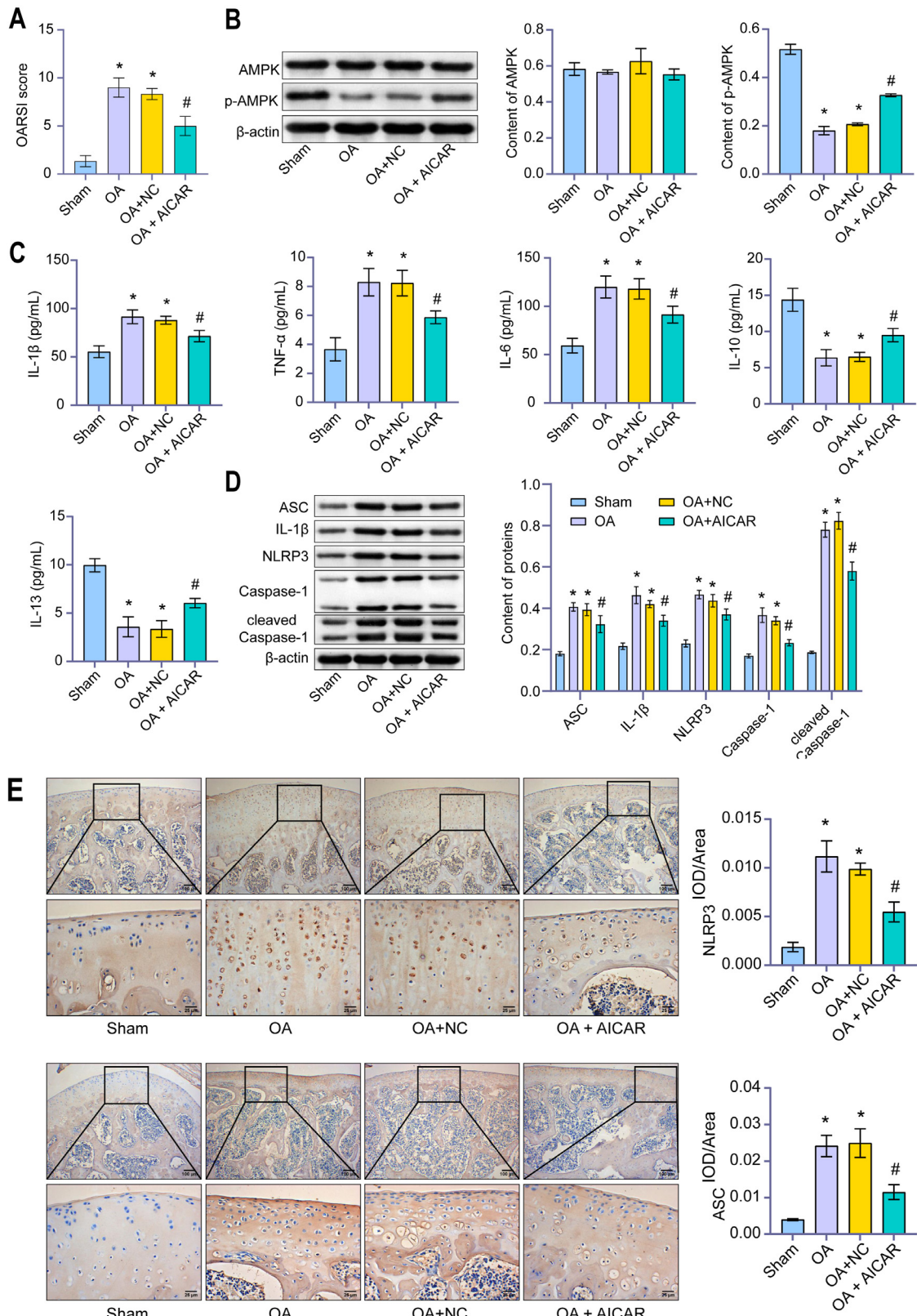
Figure 3. AMPK inhibited NLRP3 inflammatory response of OA chondrocytes. (A) OARSI score. AICAR reversed the increased of OARSI score of rats induced by OA. (B) Content of AMPK and p-AMPK were detected by western blot. After treatment with AICAR, the expression of p-AMPK increased in chondrocytes of rats induced by OA, but there was no significant difference in AMPK. (C) Content of IL-1β, TNF-α, IL-6, IL-10, and IL-13 were detected by ELISA. AICAR treatment significantly down-regulated the levels of IL-1β, TNF-α and IL-6, and increased the levels of IL-10 and IL-13. (D) Content of ASC, Caspase-1, IL-1β, NLRP3, and cleaved Caspase-1 were detected by western blot. AICAR treatment significantly down-regulated the above factors in OA rats. (E). IHC was applied to measure IOD/Area value. AICAR treatment significantly down-regulated NLRP3 and ASC expression. (IHC, × 400, scale bar = 25 μm; × 100, scale bar = 100 μm). *P < 0.05 vs. Sham. #P < 0.05 vs. OA + NC.
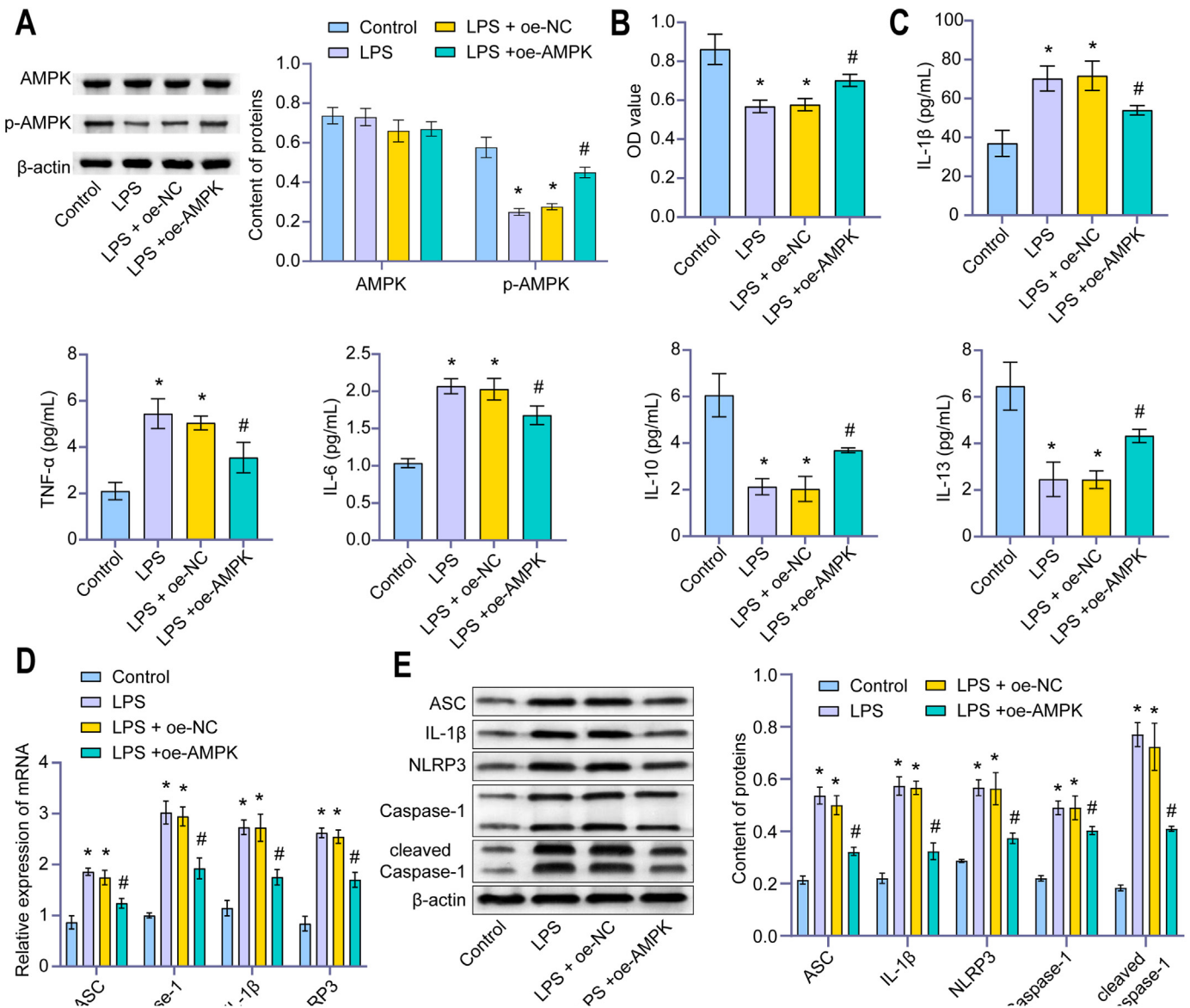
Figure 4. AMPK regulated NLRP3 inflammatory response of chondrocytes in OA to inhibit pyroptosis. (A) The content of AMPK and p-AMPK were detected by western blot. After LPS-induced human chondrocytes constructed an inflammatory model, the level of p-AMPK decreased in the LPS group. Compared with the LPS group, the level of p-AMPK in the LPS + oe-AMPK group was higher. (B) OD value (450 nm) was detected by CCK-8. In the LPS group, the cell viability decreased. Overexpression of AMPK up-regulated cell viability. (C) Content of IL-1β, TNF-α, IL-6, IL-10, and IL-13 were detected by ELISA. Overexpression of AMPK significantly up-regulated the levels of IL-10 and IL-13 and down-regulated the levels of IL-1β, TNF-α and IL-6. (D) Relative expression of ASC, Caspase-1, IL-1β, and NLRP3 were measured by qRT-PCR. (E) Content of ASC, Caspase-1, IL-1β, NLRP3, and cleaved Caspase-1 were detected by western blot. (F) The fluorescence intensity of NLRP3 and Caspase-1 were measured by IF. Overexpression of AMPK down-regulated the expression of NLRP3 inflammasomes ASC, Caspase-1, IL-1β, NLRP3, and cleaved Caspase-1. (IF, × 400, scale bar = 25 μm). (G) The apoptosis rate was detected by Flow cytometry. (H) The TUNEL-positive rate was measured by TUNEL assay. Overexpression of AMPK down-regulated the apoptosis rate and TUNEL positive rate. (TUNEL, × 400, scale bar = 25 μm). $*P < 0.05$ vs. Control. $\#P < 0.05$ vs. LPS + oe-NC.

group, Bcl-2 level were up-regulated and the levels of Bax and Caspase-3 were down-regulated in the OA + ALCAR group (Fig. 5C and D). Compared with the Sham group, the TUNEL-positive rate in the OA group increased. Compared with the OA + NC group, the TUNEL-positive rate in the OA + ALCAR group was down-regulated (Fig. 5E). IHC results showed that the Ki67 level in OA group decreased compared to the Sham group. Ki67 level in the OA + ALCAR group increased compared with the OA + NC group (Fig. 5F). These results suggested that AMPK reduces chondrocyte injury in OA rats.

4. Discussion

Our study found that LKB1 mediated the activation of AMPK in chondrocytes, and p-LKB1 decreased in chondrocytes with OA. Linear ubiquitin modification of LKB1 promoted its activity and increased AMPK activation. AMPK inhibited NLRP3 inflammatory response and pyroptosis of chondrocytes in OA and reduced cell damage. These studies suggested that linear ubiquitination of LKB1 activates the AMPK pathway and inhibits NLRP3 inflammasome response to reduce pyroptosis. Therefore, ubiquitin activation of LKB1 would be a prospective therapeutic strategy for OA treatment.

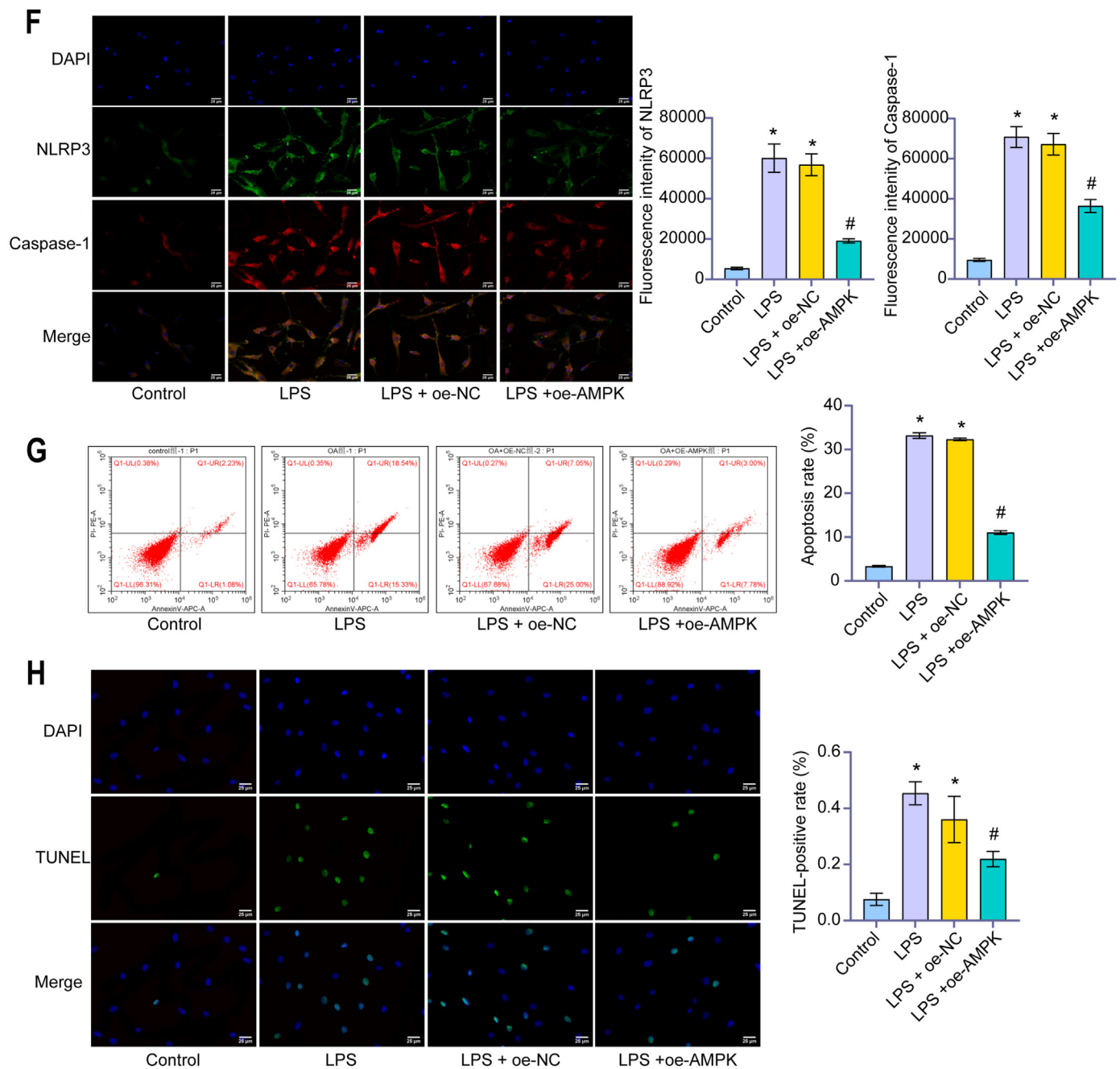AMPK has been reported to be activated by the phosphorylation of

Figure 4. (*continued*).

LKB1 [27]. Therefore, we established in OA rats or LPS-induced chondrocytes to detect whether LKB1 levels were associated with AMPK activation. Our study overexpressed LKB1 up-regulated p-AMPK protein content, down-regulated NF-κB and cleaved Caspase-1 levels, and reduced inflammatory response. Previously, it has been reported that the up-regulation of the NLRP3/Caspase-1 pathway through NF-κB is one of the key mechanisms leading to cell pyroptosis [28]. High mobility group protein 1 (HMGB1) promoted activation of NLRP3 and Caspase-8 inflammasome in acute glaucoma through the NF-κB pathway [29]. Breviscapine inhibited inflammation in pulmonary fibrosis through NF-κB/NLRP3 signaling [30]. Thus, LKB1 mediated AMPK activation in chondrocytes. However, we could not determine whether the activation of AMPK was associated with promoting LKB1 activity by ubiquitination modification. So we conducted follow-up ubiquitination modification experiments.

As the major post-translational modification of proteins, ubiquitination is related to most life activities [31]. However, the molecular mechanism behind the regulation of OA by linear ubiquitination remains unclear. The formation of linear ubiquitin chains requires the involvement of ubiquitin ligase HOIP and two regulatory subunits [32]. Ubiquitin molecules are usually covalently modified on lysine residues of substrate proteins to form polyubiquitin chains, such as K48 and K63 ubiquitin chains [32]. There is another ubiquitin chain type in cells, the linear ubiquitin chain (M1 type) [25]. In the experiment, it was found that LKB1 did not significantly precipitate in K48 and K63, but was precipitated in M1. Thus, high levels of HOIP enhanced LKB1 linear ubiquitination and increased p-AMPK expression. Together, this evidence provided strong evidence that linear ubiquitin modification promotes LKB1 activity and increases AMPK activation.

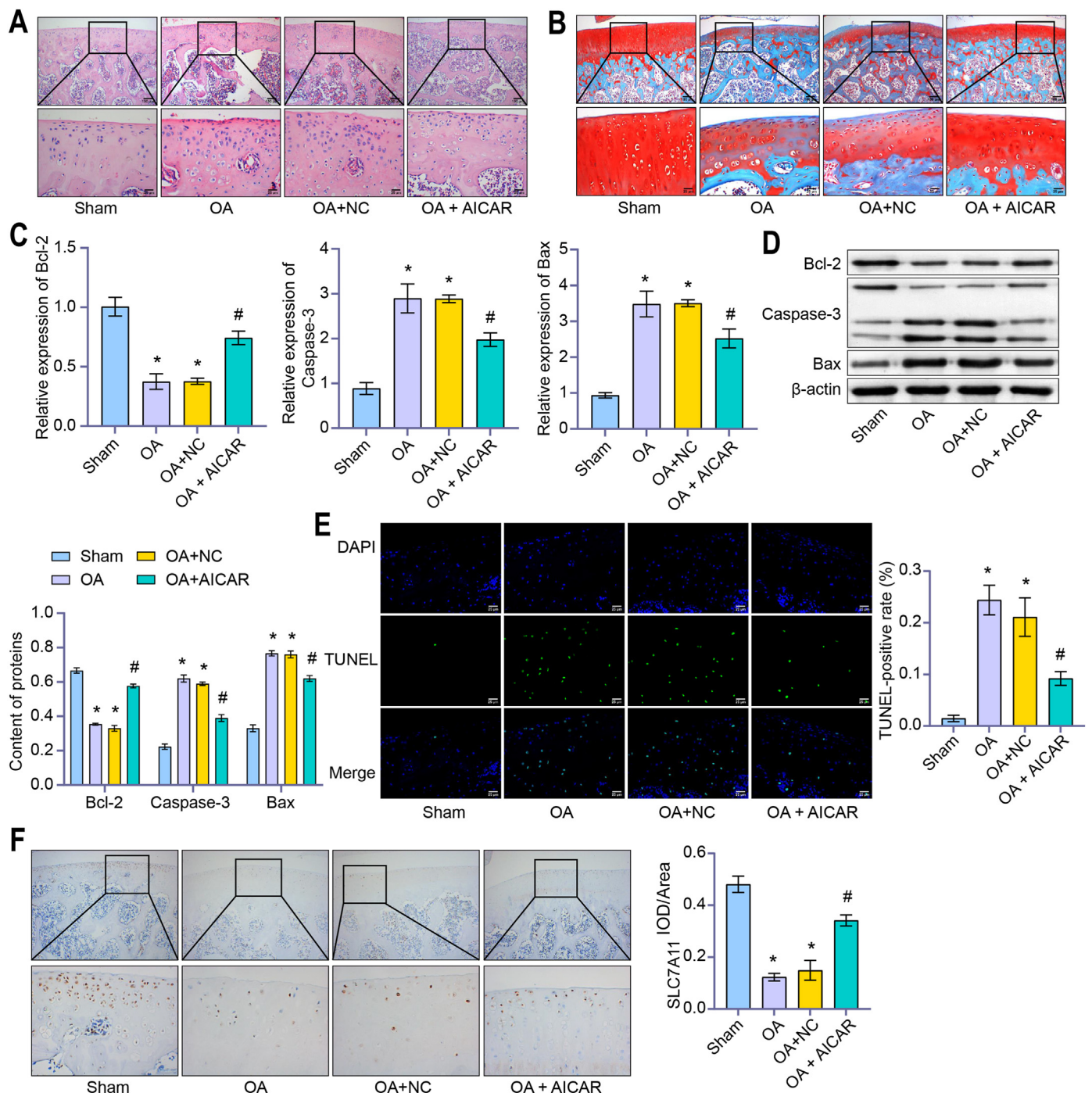AMPK is an energy sensor that regulates metabolism [33].

Figure 5. AMPK reduced chondrocyte injury in OA rats. (A) HE and (B) S–O were applied to assess the degree of tissue damage. AICAR treatment significantly alleviated tissue damage. (HE and S–O, × 400, scale bar = 25 μm; × 100, scale bar = 100 μm). (C) Relative expressions of Bcl-2, Caspase-3 and Bax were detected by qRT-PCR. (D) Content of Bcl-2, Caspase-3 and Bax were detected by western blot. Compared with the OA + NC group, Bcl-2 level were up-regulated and the levels of Bax and Caspase-3 were down-regulated in the OA + ALCAR group. (E) The TUNEL-positive rate was measured by TUNEL assay. Compared with the OA + NC group, the TUNEL-positive rate in the OA + ALCAR group was down-regulated. (TUNEL, × 400, scale bar = 25 μm). (F) IHC was applied to detect the IOD/Area value of Ki67. Ki67 level in the OA + ALCAR group increased compared with the OA + NC group. (IHC, × 400, scale bar = 25 μm; × 100, scale bar = 100 μm) *P < 0.05 vs. Sham. #P < 0.05 vs. OA + NC.

LPS-induced adipocyte inflammation is reduced through AMPK mediated pathways [34]. The expression and release of pro-inflammatory cytokines (IL-1β, IL-18 and TNF-α), NLRP3 and Caspase-3 were increased during OA inflammation [35]. Salidroside improved inflammation and oxidative stress by regulating the AMPK relative signaling pathway and reduced the content of TNF-α, IL-1β and IL-6 [36]. NLRP3 inflammasome was highly activated in the synovium of rheumatoid OA patients [37].

Therefore, to determine the relationship between AMPK and NLRP3 inflammatory response, chondrocytes of OA rats were treated with AICAR in vivo. This resulted in the down-regulation of inflammatory cytokines and NLRP3 inflammasome (ASC, Caspase-1, IL-1β, NLRP3, and cleaved Caspase-1). Thus, AMPK inhibited the inflammation of OA.

In addition to inflammation, AMPK activation also appears to reduce scoliosis, specifically alleviating OA-induced cell death. It has been found

that activation of autophagy by the ROS-AMPK-mTOR axis protects Leydig cells from pyroptosis [14]. Diosgenin can activate AMPK/Nrf2 to inhibit the pyroptosis of myometrial microvascular endothelial cells (MMEC) [38]. We found overexpression of AMPK down-regulated the expression of NLRP3 inflammasomes ASC, Caspase-1, IL-1β, NLRP3, and cleaved Caspase-1. NLRP3 inflammasomes induce pyroptosis by cleaving gasdermin D (GSDMD) into its active form, GSDMD-N, and forming pores in cell membranes [39]. Increased activation of NLRP3 and pyroptosis induced by GSDMD-N can aggravate inflammation and increase the level of ROS to aggravate neuropathic pain [40]. Our data are consistent with existing studies. Overexpression of AMPK up-regulated cell activity and reduced NLRP3 inflammatory response to inhibit pyroptosis.

After confirming the alleviating effect of LKB1/AMPK on OA disease, we further carried out histopathological observation. It has been found that after trichosanthin (TCS) treatment, Ki67-positive cells number decreased significantly, and cleaved-Caspase-3 level increased, inhibited the proliferation of cervical cancer cells [41]. AICAR treatment in rats also significantly alleviated tissue damage and cell apoptosis in rats with OA, and up-regulated Ki67 level. Our study further confirms that activation of the AMPK pathway reduces chondrocyte damage and scoria in OA.

5. Conclusion

Our present study highlighted the importance of the LKB1/AMPK pathway in NLRP3 inflammatory body response and chondrocyte injury. Linear ubiquitin modification of LKB1 promoted its activity and increased AMPK activation. AMPK inhibited NLRP3 inflammatory response and pyroptosis of chondrocytes in OA and reduced cell damage. Activation of the AMPK pathway by linear ubiquitination modification of LKB1 may be a potential target for OA treatment.

Author contributions

Xu Cao, Song Wu: Conceptualization, Methodology, Software, **Yang Chen, Yiheng Liu, Kai Jiang**: Data curation, Writing- Original draft preparation, **Zi Wen**: Visualization, Investigation, **Xu Cao, Song Wu**: Supervision, **Yang Chen, Yiheng Liu, Kai Jiang, Zi Wen**: Software, Validation, **Yang Chen**: Writing- Reviewing and Editing, All the authors above approved the version of the manuscript to be published.

Declaration of competing interest

The authors declare that they have no known competing financial interests or personal relationships that could have appeared to influence the work reported in this paper.

Acknowledgments

References

[1] Mandl LA. Osteoarthritis year in review 2018: clinical. Osteoarthritis Cartilage 2019;27(3):359–64.

[2] Abramoff B, Caldera FE. Osteoarthritis: Pathology, Diagnosis, and Treatment Options. Med Clin North Am 2020;104(2):293–311.

[3] Zheng L, Zhang Z, Sheng P, Mobasheri A. The role of metabolism in chondrocyte dysfunction and the progression of osteoarthritis. Ageing Res Rev 2021;66:101249.

[4] Shen S, Wu Y, Chen J, Xie Z, Huang K, Wang G, et al. CircSERPINE2 protects against osteoarthritis by targeting miR-1271 and ETS-related gene. Ann Rheum Dis 2019; 78(6):826–36.

[5] Kim DY, Lim SG, Suk K, Lee WH. Mitochondrial dysfunction regulates the JAK-STAT pathway via LKB1-mediated AMPK activation ER-stress-independent manner. Biochem Cell Biol 2020;98(2):137–44.

[6] Chen Y, Wu YY, Si HB, Lu YR, Shen B. Mechanistic insights into AMPK-SIRT3 positive feedback loop-mediated chondrocyte mitochondrial quality control in osteoarthritis pathogenesis. Pharmacol Res 2021;166:105497.

[7] Carling D. AMPK signalling in health and disease. Curr Opin Cell Biol 2017;45: 31–7.

[8] Wang J, Li J. AMPK: implications in osteoarthritis and therapeutic targets. Am J Transl Res 2020;12(12):7670–81.

[9] Petursson F, Husa M. Linked decreases in liver kinase B1 and AMP-activated protein kinase activity modulate matrix catabolic responses to biomechanical injury in chondrocytes. Arthritis Res Ther 2013;15(4).

[10] Ji J, Xue TF, Guo XD, Yang J, Guo RB, Wang J, et al. Antagonizing peroxisome proliferator-activated receptor γ facilitates M1-to-M2 shift of microglia by enhancing autophagy via the LKB1-AMPK signaling pathway. Aging Cell 2018; 17(4):e12774.

[11] Feng X, Pan J, Li J, Zeng C, Qi W, Shao Y, et al. Metformin attenuates cartilage degeneration in an experimental osteoarthritis model by regulating AMPK/mTOR. Aging (Albany NY) 2020;12(2):1087–103.

[12] Yang F, Qin Y. Metformin Inhibits the NLRP3 Inflammasome via AMPK/mTOR-dependent Effects in Diabetic Cardiomyopathy. Int J Biol Sci 2019;15(5):1010–9.

[13] Yao RQ, Ren C, Xia ZF, Yao YM. Organelle-specific autophagy in inflammatory diseases: a potential therapeutic target underlying the quality control of multiple organelles. Autophagy 2021;17(2):385–401.

[14] Li MY, Zhu XL, Zhao BX, Shi L, Wang W, Hu W, et al. Adrenomedullin alleviates the pyroptosis of Leydig cells by promoting autophagy via the ROS-AMPK-mTOR axis. Cell Death Dis 2019;10(7):489.

[15] Tong L, Yu H, Huang X, Shen J, Xiao G, Chen L, et al. Current understanding of osteoarthritis pathogenesis and relevant new approaches. Bone Res 2022;10(1):60.

[16] Wang Y, Gao W, Shi X, Ding J, Liu W, He H, et al. Chemotherapy drugs induce pyroptosis through caspase-3 cleavage of a gasdermin. Nature 2017;547(7661): 99–103.

[17] Makoni NJ, Nichols MR. The intricate biophysical puzzle of caspase-1 activation. Arch Biochem Biophys 2021;699:108753.

[18] Fang Y, Tian S, Pan Y, Li W, Wang Q, Tang Y, et al. Pyroptosis: A new frontier in cancer. Biomed Pharmacother 2020;121:109595.

[19] Zeng C, Wang R, Tan H. Role of pyroptosis in cardiovascular diseases and its therapeutic implications. Int J Biol Sci 2019;15(7):1345–57.

[20] Zu Y, Mu Y. Icariin alleviates osteoarthritis by inhibiting NLRP3-mediated pyroptosis. J Orthop Surg Res 2019;14(1).

[21] Gerlach B, Cordier SM, Schmukle AC, Emmerich CH, Rieser E, Haas TL, et al. Linear ubiquitination prevents inflammation and regulates immune signalling. Nature 2011;471(7340):591–6.

[22] Kamekura S, Hoshi K, Shimoaka T, Chung U, Chikuda H, Yamada T, et al. Osteoarthritis development in novel experimental mouse models induced by knee joint instability. Osteoarthritis Cartilage 2005;13(7):632–41.

[23] Wang J, Fang L, Ye L, Ma S, Huang H, Lan X, et al. miR-137 targets the inhibition of TCF4 to reverse the progression of osteoarthritis through the AMPK/NF-κB signaling pathway. Biosci Rep 2020;40(6).

[24] Giri S, Nath N, Smith B, Viollet B, Singh AK, Singh I. 5-aminoimidazole-4-carboxamide-1-beta-4-ribofuranoside inhibits proinflammatory response in glial cells: a possible role of AMP-activated protein kinase. J Neurosci 2004;24(2): 479–87.

[25] Wang J, Fang L. miR-137 targets the inhibition of TCF4 to reverse the progression of osteoarthritis through the AMPK/NF-κB signaling pathway. Biosci Rep 2020;40(6).

[26] Pritzker KP, Gay S, Jimenez SA, Ostergaard K, Pelletier JP, Revell PA, et al. Osteoarthritis cartilage histopathology: grading and staging. Osteoarthritis Cartilage 2006;14(1):13–29.

[27] Zhang YL, Guo H, Zhang CS, Lin SY, Yin Z, Peng Y, et al. AMP as a low-energy charge signal autonomously initiates assembly of AXIN-AMPK-LKB1 complex for AMPK activation. Cell Metab 2013;18(4):546–55.

[28] Jiang S, Zhang H, Li X, Yi B, Huang L, Hu Z, et al. Vitamin D/VDR attenuate cisplatin-induced AKI by down-regulating NLRP3/Caspase-1/GSDMD pyroptosis pathway. J Steroid Biochem Mol Biol 2021;206:105789.

[29] Chi W, Chen H, Li F, Zhu Y, Yin W, Zhuo Y. HMGB1 promotes the activation of NLRP3 and caspase-8 inflammasomes via NF-κB pathway in acute glaucoma. J Neuroinflammation 2015;12:137.

[30] Peng L, Wen L, Shi QF, Gao F, Huang B, Meng J, et al. Scutellarin ameliorates pulmonary fibrosis through inhibiting NF-κB/NLRP3-mediated epithelial-mesenchymal transition and inflammation. Cell Death Dis 2020;11(11):978.

[31] Varshavsky A. The Ubiquitin System, Autophagy, and Regulated Protein Degradation. Annu Rev Biochem 2017;86:123–8.

[32] Jahan AS, Elbæk CR, Damgaard RB. Met1-linked ubiquitin signalling in health and disease: inflammation, immunity, cancer, and beyond. Cell Death Differ 2021; 28(2):473–92.

[33] Lyons CL, Roche HM. Nutritional Modulation of AMPK-Impact upon Metabolic-Inflammation. Int J Mol Sci 2018;19(10):3092.

[34] Jung TW, Park HS, Choi GH, Kim D, Lee T. β-aminoisobutyric acid attenuates LPS-induced inflammation and insulin resistance in adipocytes through AMPK-mediated pathway. J Biomed Sci 2018;25(1):27.

[35] Li W, Wang Y, Tang Y, Lu H, Qi Y, Li G, et al. Quercetin Alleviates Osteoarthritis Progression in Rats by Suppressing Inflammation and Apoptosis via Inhibition of IRAK1/NLRP3 Signaling. J Inflamm Res 2021;14:3393–403.

[36] Hu R, Wang MQ, Ni SH, Wang M, Liu LY, You HY, et al. Salidroside ameliorates endothelial inflammation and oxidative stress by regulating the AMPK/NF-κB/

NLRP3 signaling pathway in AGEs-induced HUVECs. Eur J Pharmacol 2020;867: 172797.

[37] Guo C, Fu R, Wang S, Huang Y, Li X, Zhou M, et al. NLRP3 inflammasome activation contributes to the pathogenesis of rheumatoid arthritis. Clin Exp Immunol 2018; 194(2):231–43.

[38] Ran X, Yan Z, Yang Y, Hu G, Liu J, Hou S, et al. Dioscin Improves Pyroptosis in LPS-Induced Mice Mastitis by Activating AMPK/Nrf2 and Inhibiting the NF-κB Signaling Pathway. Oxid Med Cell Longev 2020;2020:8845521.

[39] He WT, Wan H, Hu L, Chen P, Wang X, Huang Z, et al. Gasdermin D is an executor of pyroptosis and required for interleukin-1β secretion. Cell Res 2015;25(12): 1285–98.

[40] Li J, Tian M, Hua T, Wang H, Yang M, Li W, et al. Combination of autophagy and NFE2L2/NRF2 activation as a treatment approach for neuropathic pain. Autophagy 2021;17(12):4062–82.

[41] Zhu C, Zhang C, Cui X, Wu J, Cui Z, Shen X. Trichosanthin inhibits cervical cancer by regulating oxidative stress-induced apoptosis. Bioengineered 2021;12(1): 2779–90.